Cover Page

Universiteit Leiden

Author: Deventer, Sjoerd van
Title: Tracking the big ones : novel dynamics of organelles and macromolecular complexes during cell division and aging
Issue Date: 2015-10-21

Chapter Five

Chapter 5:

How is the proteasome degraded?

Sjoerd J. van Deventer[1], Victoria Menendez-Benito[1],
Martje Erkelens[1], Fred van Leeuwen[2], Jacques Neefjes[1]

Manuscript in preparation

5

[1] Division of Cell Biology 2 and
[2] Division of Gene Regulation,
Netherlands Cancer Institute, Amsterdam, The Netherlands

Abstract

To maintain cellular fitness and functionality throughout its lifetime, a cell needs to maintain the quality of its proteins. Cells therefore employ the ubiquitin-proteasome system (UPS) to specifically degrade damaged proteins. Still, protein damage tends to accumulate during cellular aging and is implicated in several age-related diseases, which suggests limiting UPS activity. One reason for limiting UPS activity may be that proteasomes get damaged and then become less effective. Therefore, analogous to damaged proteins, one would expect that damaged proteasomes would be specifically cleared from the cell. The scope and mechanism of such a proteasome quality control system, however, remain to be determined. In this Chapter, we present arguments for lysosomal degradation of proteasomes in budding yeast and mammalian HeLa cells. Also, our data is consistent with specificity towards damaged proteasomes, as a quality control system requires. Our observations may thus represent the first sketches of a quality control system for the proteasome. A deeper understanding of such system may yield new insights in aging and the treatment of age-related diseases.

Introduction

To survive as a single cell or to function within a multicellular organism, a cell needs to maintain its fitness and functionality throughout its lifetime. An important aspect thereof is the maintenance of a functional pool of cellular proteins. To keep their proteins in optimal condition, cells continuously synthesize new proteins and repair or degrade damaged proteins. In fact, synthesis, repair and degradation processes keep the pool of cellular proteins in a constant flux. Tight regulation of these processes allows the cell to maintain a functional pool of proteins under a variety of different conditions, like altering nutrient conditions, stress conditions and signaling [1,2]. Despite the cells efforts to maintain protein fitness, damaged proteins do accumulate during the lifetime of a cell. Accumulation of damaged proteins is a hallmark of cellular aging and has been implicated in several age-related diseases [3,4].

To prevent harmful accumulation of damaged proteins, cells have to degrade proteins that cannot be repaired. Degradation of damaged proteins is mediated by two degrading entities; the lysosome and the proteasome [5]. The lysosome is a membrane-enclosed compartment filled with proteases. Proteins to be degraded by this compartment can be targeted by a process called autophagy, of which several types exist. The most common type is macro-autophagy, which involves the formation of a double membrane structure (the autophagosome) around the substrate proteins. The autophagosome subsequently fuses with the lysosome followed by degradation of its content [6]. Another type of autophagy is micro-autophagy, which entails the endocytosis of substrates by the lysosome [7]. Autophagy in general was long considered to be a non-specific bulk degradation process of (damaged) cytoplasmic proteins and organelles [8]. However, increasing specificity and diversity is assigned to this process, such as the specific degradation of ribosomes and mitochondria [8,9].

The other protein degrading entity in cells is the proteasome. The proteasome is a protein complex that can be divided into two sub-complexes; the 20S core particle (20S) and one or two 19S regulatory particles (19S). The 20S and the 19S together form

the active 26S proteasome [10]. The 20S is the degrading part of the proteasome and is formed by the stacking of four protein rings (each containing seven subunits) into a tube-shaped structure. Inside this tube, the catalytic activity is conveyed by two sets of three catalytically active subunits [11]. For substrate proteins to be degraded inside the 20S they need to be unfolded and pushed into the 20S tube, a task mediated by the 19S complex that caps one or both ends of the 20S tube. The 19S complex recognizes proteasome substrates by their poly-ubiquitin tail, which is removed before the substrate is degraded [12]. Poly-ubiquitination of substrate proteins is mediated by an enzymatic cascade of ubiquitin-activating (E1), ubiquitin-conjugating (E2) and ubiquitin-ligating (E3) enzymes. Together, these enzymes form the ubiquitination machinery, which selectively targets (damaged) proteins for degradation by the proteasome [13]. The proteasome and the ubiquitination machinery together form the ubiquitin-proteasome system (UPS). By selective degradation of damaged proteins, the UPS plays an important role in the cell's defense against the accumulation of damaged proteins during its lifetime [14].

The accumulation of damaged proteins during cellular aging suggests that the degrading activity of the cell can become limiting and correlates with the decrease in proteasome activity observed in several aging model organisms [15–18]. Decreasing proteasome activity is suggested to be a causative factor in the aging process [19,20] and enhanced activity of the proteasome is found to correlate with longer longevity in several organisms including humans [21,22]. These observations fuel a growing interest in ways to enhance proteasome activity as a potential treatment for neurodegenerative and other age-related diseases [4]. Finding the causes underlying this age-related decrease in proteasome activity, may provide new modalities of treatment for age-related diseases.

Several factors are proposed to play a role in the age-related decrease of proteasome activity, including decreased proteasome levels, altered proteasome conformation or decreased efficiency of proteasomes. Decreasing proteasome levels are observed in several model organisms, often deduced from lower expression of proteasome subunits [15,17]. The reason for this counterintuitive decrease in expression levels is unclear. Conformational changes in proteasomes during aging are observed in *Drosophila* and budding yeast, which show an age-dependent decline in 26S proteasomes in favor of the less active 20S forms [18,23]. In human lymphocytes on the other hand, levels and conformation of the proteasome are stable during aging and still they show a decreasing proteasome activity. This decreasing activity correlates with an increasing number of post-translational modifications of the proteasomes (glycation and conjugation with lipid peroxidation products), suggesting that these modifications damage the proteasome and make it less efficient [24]. A model in which damage to the proteasome compromises its efficiency is also consistent with several *in vitro* and *in vivo* studies showing decreased proteasome activity upon treatment with oxidizing agents like nitric oxide [15,25]. Although none of these studies shows the actual oxidative damage to the proteasome, it is likely that proteasomes obtain oxidative damage during their lifetime, given their long half-life [26–28] and the increased oxidative stress in aging cells as a result of malfunctioning mitochondria [29]. Another reason for age-dependent decreasing efficiency of the proteasome may be that they may get 'clogged' by certain substrates [15].

To prevent the accumulation of less functional proteasomes, cells are expected to employ a 'proteasome quality control system'. The action of such a quality control system would be of particular importance for long-lived non-dividing cells, like neurons. This type of cells cannot simply 'dilute' their malfunctioning proteasomes by cell division and since

5

they are long-lived they will need exquisite proteasome activity to maintain proteome fitness during their entire lifetime. The relevance of optimal proteasome activity in these cells is highlighted by the accumulation of damaged proteins in many neurodegenerative disorders [3]. Elucidation of the mechanism involved in proteasome quality control may therefore yield important insights in the pathology of neurodegenerative and other age-related diseases.

Two issues should be considered for proteasome quality control; recognition of damaged proteasomes and a degradation mechanism. Nothing is known about the first, though there are hints for mechanisms involved in the latter. The first evidence for *in vivo* degradation of proteasomes came from pulse-chase experiments in HeLa cells with tritium labeled leucine. In this study a half-life of 5-6 days was found for the 19S 'prosome', which was later identified as the 20S core particle [26,30]. Pulse-chase experiments in adult rats yielded half-lifes ranging from 4 to 15 days for the 20S particle in the liver and 8 days for the 20S particle in rat brain [27,28,31]. These pulse-chase experiments show that the 20S proteasome is remarkably stable in both dividing (HeLa) and non-dividing (rat brain and liver) cells, but do not provide mechanistic insights.

The first mechanistic insights came from a study with isolated lysosomes from the liver of adult rats. Incubation of purified proteasomes with broken rat lysosomes at pH 5 at 37°C showed that proteasomes can be degraded under lysosomal conditions. Furthermore, proteasomes were detected in lysosomes isolated from starved and/or leupeptin treated rats, whereas they could not be detected in lysosomes of normally fed rats [28]. This suggests that proteasomes can be degraded by lysosomes *in vivo* and the correlation with starvation may suggest that autophagy plays a role in the delivery of the proteasome to the lysosome. Proteasome delivery to the lysosome was shown in an *in vitro* model for micro-autophagy, which may be indicative for the involvement of micro-autophagy *in vivo* [28].

In this Chapter, we extend the above findings to model systems more suitable for in-depth analysis of the mechanisms underlying proteasome degradation; budding yeast and HeLa cells. In both model systems we find indications for lysosomal degradation of the proteasome and our findings in HeLa cells are consistent with autophagic delivery of damaged proteasomes to the lysosome. Our findings may thus provide the first sketches of a proteasome quality control system.

Results

Proteasomes can be detected in yeast vacuoles, but degradation cannot be detected by RITE

To study degradation of proteasomes in budding yeast, the catalytically active β1 subunit (Pre3) of the proteasome was tagged endogenously with a GFP tag. β1-GFP is efficiently and quantitatively incorporated in functional 20S core particles [32]. A potential role of the vacuole, the yeast homologue of the lysosome, is best studied in starved yeast cells as they have one big central vacuole. Electron microscopy after a five-day starvation showed immunogold labeling of GFP in the vacuolar compartment (Fig1A). GFP was found both in the vacuolar lumen and in membrane-enclosed structures that may resemble the final stages of autophagosomes. Analogous to the findings in rat livers, this suggests a role for the vacuole in the degradation of the proteasome and a possible role for autophagy.

To further study the potential factors involved in proteasome degradation, the β1 subunit
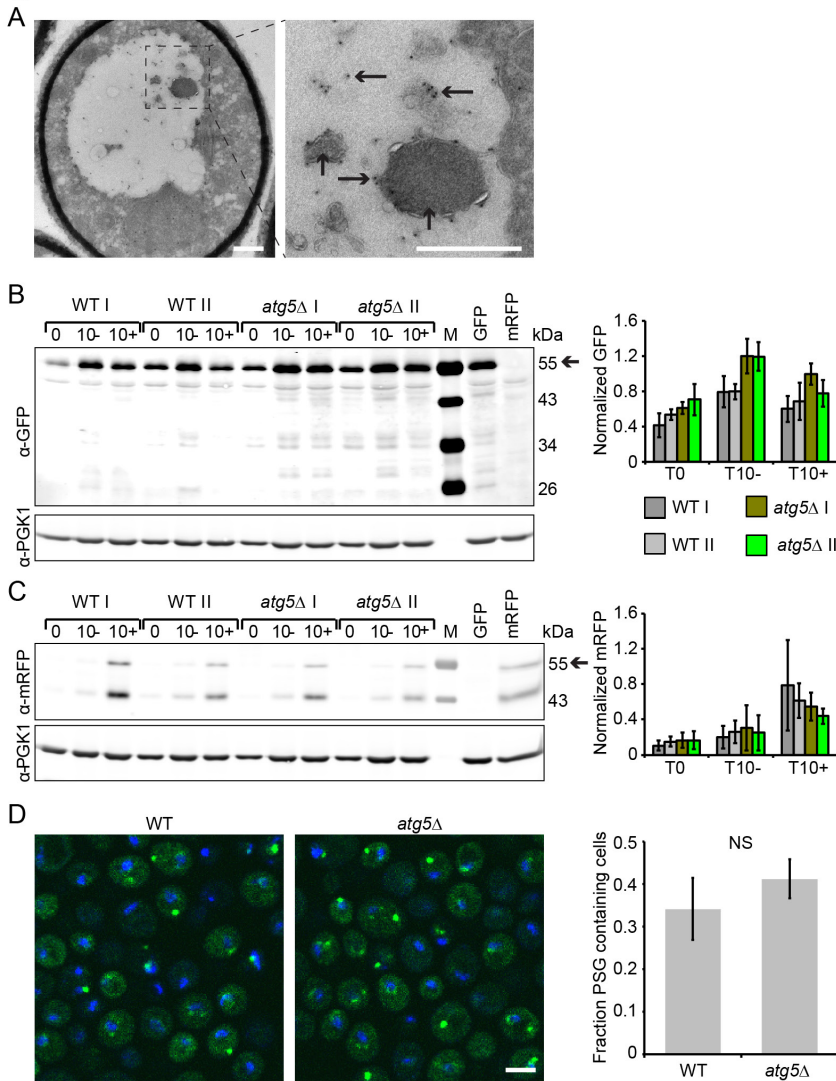
Figure 1

Figure1: Proteasomes can be detected in yeast vacuoles, but degradation cannot be detected by RITE
A) Immunolocalization of yeast 20S proteasomes by EM in starved yeast cells expressing β1-GFP. Samples were stained with a primary antibody against GFP and a secondary antibody coupled to 10-nm gold particles. Examples of gold particles are highlighted with a horizontal arrow. Potential remainders of autophagosomes are highlighted with a vertical arrow. Scale bar: 500 nm. B) Detection of old proteasomes (β1-GFP, ~55 kDa) in total lysates of two WT and two autophagy-deficient (*atg5Δ*) yeast strains expressing β1-RITE. Samples were taken after 2 days in starvation (T0), when the recombination was induced and 10 days later in both non-recombined (T10-) and recombined (T10+) cultures. Full length β1-GFP is indicated with an arrow and the housekeeping enzyme Pgk1 was used as a loading control. Values and standard deviations of the quantification are based on a biological triplicate and normalized to a strain expressing β1-GFP. C) The same samples used for B) were also probed and quantified for new proteasomes (β1-mRFP, ~55 kDa and a degradation band at ~43 kDa). D) Single plane confocal images of 5 day starved β1-GFP expressing WT and autophagy-deficient cells. Hoechst was used as nuclear counter staining. Scale bar: 5 µm. The prevalence of cells containing PSG is quantified by cell counting. Values and standard deviations are based on a biological triplicate.

of the yeast proteasome was endogenously tagged with a fluorescent Recombination-Induced Tag Exchange (RITE) cassette. The RITE cassette behind the β1 gene results in a fusion protein, which initially expresses as β1-GFP. However, an irreversible hormone-induced DNA recombination event results in expression of β1-mRFP. This system defines an old population of proteasomes, produced before the recombination event (green), and a new population produced after the recombination event (red) [33]. Degradation of the proteasome can now be detected by a decrease in the old (GFP-tagged) population of proteasomes (like in a classical pulse-chase), whereas synthesis of proteasomes can be addressed by an increasing level of new (mRFP-tagged) proteasomes.

Since cell divisions will cause a decrease in the old protein population by dilution, degradation of the old proteasome pool can best be detected in conditions with little or no proliferation. These conditions can be met by growing a liquid yeast culture until the carbon source gets depleted and cells enter a starvation induced quiescent state [34]. In our experiments, the recombination of the RITE cassette was induced after a two day growth of a liquid culture, when cell division has almost ceased (Fig S1). At this time point ~5% of the cells had already undergone (non-induced) recombination, whereas adding the hormone β-estradiol in these conditions resulted in recombination in ~90% of the cells (Fig S1).

To assess a role for autophagy in proteasome degradation, the proteasome was RITE tagged in two WT and two autophagy-deficient (atg5Δ) yeast strains. Yeast strains lacking Atg5, are deficient for macro-autophagy and hampered in micro-autophagy [7]. After a two day starvation of WT and atg5Δ cells, recombination was induced and the cells were kept in this low-dividing state for an additional 10 days to allow them to degrade their proteasomes. A parallel culture without induction of recombination served to assess the changes in overall proteasome levels. Recombination and growth characteristics are not significantly different between both strains, which allows their comparison (Fig S1).

The levels of old (GFP-tagged) proteasome were assessed by the levels of β1-GFP (~55 kDa) in cell lysates made at the time of recombination (T0) and 10 days after that, either with (T10+) or without (T10-) recombination (Fig 1B). The housekeeping enzyme Pgk1 served as a loading control. The β1-GFP levels did not show a decrease between T0 and T10+ for either WT or atg5Δ cells, indicating that there was no detectable proteasome degradation. Neither was fast proteasome degradation detected by the accumulation of free GFP (~25 kDa), as was previously reported for the starvation-induced degradation of ribosomal subunits by autophagy [9,35]. The β1-GFP levels do show that overall proteasome levels were higher for atg5Δ cells in both T0 and T10-, which may suggest that the loss of autophagic activity in these cells was compensated by increased proteasome activity. Also, comparing the β1-GFP levels of T0 with T10- shows that overall proteasome levels increase during the starvation process in both WT and atg5Δ cells. Increasing overall proteasome levels in the population of cells that did not perform the recombination (~10%) may also explain the slight increase in β1-GFP levels observed between T0 and T10+. Detection of β1-mRFP (~55kDa and a degradation band at ~43 kDa) in the same lysates yielded information about the synthesis of new proteasomes during starvation (Fig 1C). As expected, the β1-mRFP levels were low for T0 and T10- and the higher levels in T10+ are consistent with the overall increase in proteasome levels. Overall, we can conclude that RITE technology was not able to detect degradation of the proteasome in this system. This can be due to insufficient sensitivity of this technology or the absence of proteasome degradation in starved yeast cells.

A very slow, or even absent, degradation of the proteasome in starving yeast cells may be caused by the presence of Proteasome Storage Granules (PSGs). These starvation-induced cytoplasmic clusters of proteasomes were found in respectively ~35% of the WT and 40% of the *atg5Δ* cells (Fig 1D) and suggested to be important for proteasome storage under starvation conditions [36]. Our data is consistent with a model in which proteasomes in PSGs are protected from degradation. Given this hypothesis, we decided not to pursue the study of proteasome degradation in starved budding yeast and move on to another model system; mammalian cell lines.
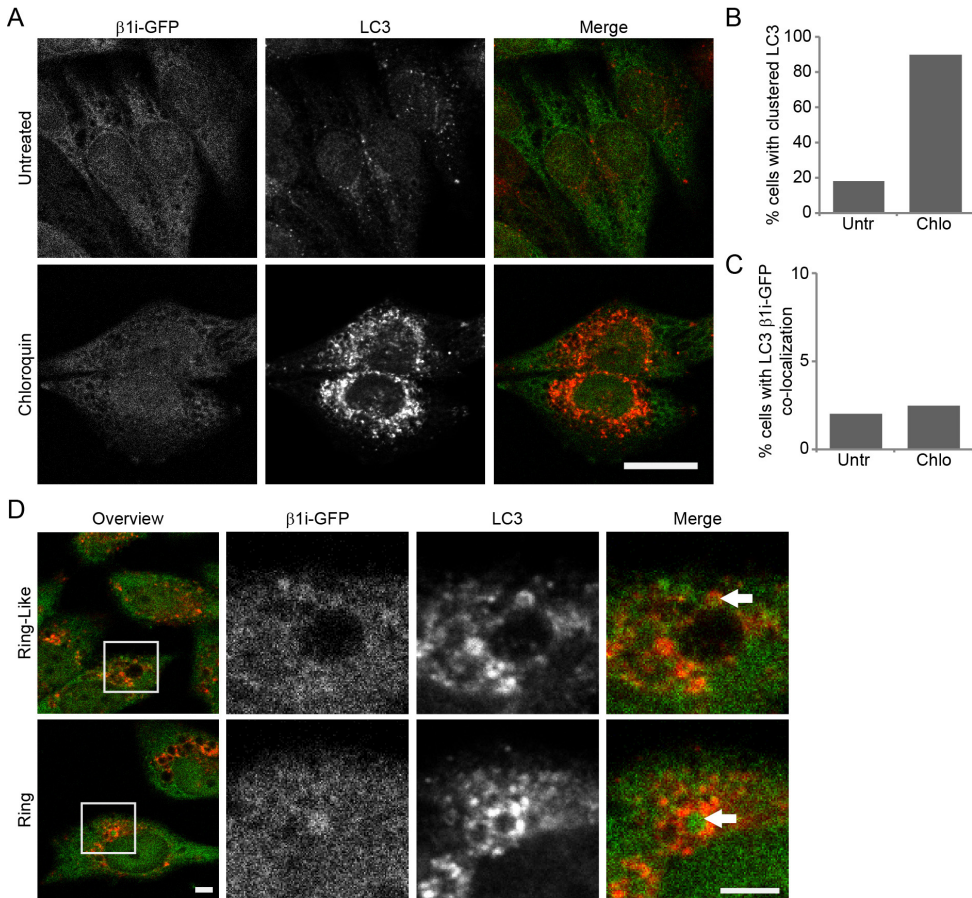
Figure 2

5

Figure 2: Proteasomes can be detected in autophagosomes in HeLa cells
A) Single plane confocal images of methanol-fixed β1i-GFP overexpressing HeLa cells either treated or non-treated for 16h with chloroquin to inhibit lysosomal degradation. β1i-GFP was visualized by direct fluorescence and immunofluorescent staining was used to visualize LC3, which marks autophagosomal membranes. Scale bar: 10 µm. B) The percentage of cells with a clustered LC3 phenotype was scored in the experiment depicted in panel A. 150 cells were scored per condition. C) The percentage of cells with one or more co-localization events between LC3 and the proteasome was scored in the experiment depicted in A). A co-localization event is defined as proteasome enrichment surrounded (Ring) or partially surrounded (Ring-like) by LC3 staining. 150 cells were scored per condition. D) Representative confocal images of the two types of proteasome-LC3 co-localization found: ring-like and ring. Scale bar: 10 µm.

Proteasomes are substrates of autophagosomes in HeLa cells

To visualize proteasomes in HeLa cells, a GFP-tagged β1i (LMP2) (immuno-) proteasome subunit was stably over expressed. β1i-GFP is efficiently and quantitatively incorporated in the 20S core particle and thus a bona fide marker for proteasome localization [37]. If the proteasome is indeed targeted for degradation by autophagy, one would expect to find co-localization with autophagosomal membranes. These membranes can be visualized by immuno-fluorescent staining for LC3 [38], which showed a punctate pattern in untreated HeLa cells (Fig 2A). In these cells, one or two LC3 β1i-GFP co-localization events were observed in ~2% of the cells (Fig 2C). A co-localization event is defined as proteasome enrichment surrounded (Ring) or partially surrounded (Ring-like) by LC3 staining (Fig 2D). Ring and ring-like co-localization may represent different stages in the internalization of proteasomes in the autophagosome. The low incidence of this co-localization can either be caused by a low incidence of proteasome degradation or by the high rate of the autophagic flux. Autophagosomes and their internalized substrates have a relatively short half-life, as they will fuse with lysosomes and thereby get degraded. This short half-life decreases the chance of finding co-localization of autophagosomes and their substrates, but can be prolonged by inhibition of lysosomal degradation. Lysosomal degradation can be inhibited by the addition of chloroquin [39], which neutralizes the lysosomal pH and results in a strong increase in the number and clustering of LC3 positive vesicles (Fig 2A-B). Despite a strong increase in LC3 positive vesicles, the number of cells with LC3 β1i-GFP co-localization increased very modestly from ~2% under untreated conditions to ~3% after a 16h treatment with chloroquin (Fig 2C). This modest increase suggests that the uptake of the proteasome by autophagosomes is a process with a low flux under normal conditions.

Proteasome uptake by autophagosomes is induced by covalent proteasome inhibitors

If the observed uptake of proteasomes in autophagosomes is part of a quality control system, one would expect that damage to the proteasome would increase the flux of this process. To damage proteasomes, cells were treated with the covalent proteasome inhibitor MV151, which targets an active site of proteasomes and has a fluorescent group [40]. HeLa cells overexpressing β1i-GFP were treated with MV151 for 2h and proteasome localization was observed 16h after thoroughly washing the cells. Treatment with MV151 alone resulted in a modest increase in LC3 β1i-GFP co-localization, though an additional 16h treatment with chloroquin resulted in a strong increase (Fig 3AC). This suggests an increased autophagic flux of the proteasome upon inhibition with MV151. Other covalent proteasome inhibitors, like epoxomycine and lactacystin had a similar effect (data not shown). Unlike these inhibitors, MV151 has a fluorescent group, which allows visualization of the inhibited proteasome. The presence of MV151 within the ring or ring-like LC3 staining showed the internalization of mature inhibited proteasomes (Fig 3B). However, since MV151 signal co-localized with β1i-GFP throughout the cell we cannot tell whether this internalization is specific (excluding not inhibited proteasomes). The overall co-localization of MV151 with β1i-GFP, suggests that the (partial) proteasome inhibition by MV151 not necessarily renders the proteasome useless for the cell. Still our data suggests an increased autophagic flux of the proteasome following covalent inhibition.
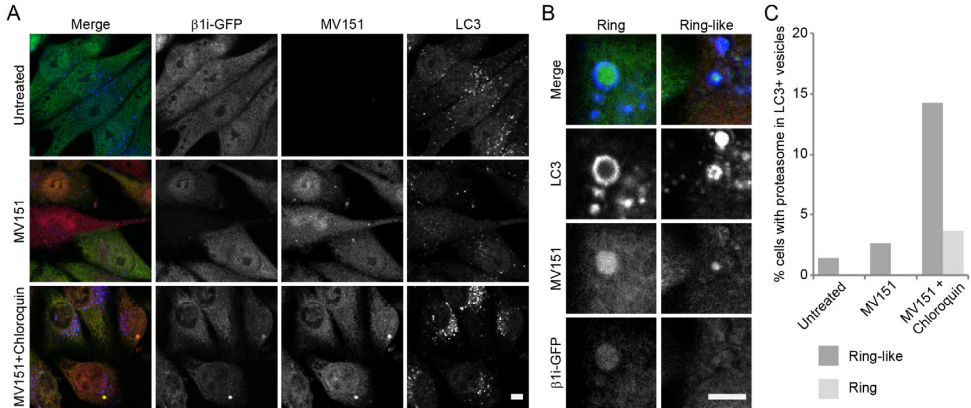
Fig 3

Figure 3: Proteasome uptake by autophagosomes is induced by covalent proteasome inhibition
A) Single plane confocal images of formaldehyde-fixed β1i-GFP overexpressing HeLa cells 16h after a 2h treatment with the covalent and fluorescent proteasome inhibitor MV151. β1i-GFP and MV151 are visualized by direct fluorescence and LC3 by immunofluorescent staining. Chloroquin was added to inhibit lysosomal degradation. Scale bar: 10 μm. B) Single plane confocal images of ring-like and ring LC3 staining around the proteasome. Scale bar: 10 μm. C) Prevalence of cells showing ring and rind-like LC3 staining around the proteasome 16h after the MV151 pulse of the experiment shown in A). Values are based on ~150 cells per condition.

Inhibited proteasomes are degraded

The data presented above suggests that the degradation of the proteasome can be enhanced by its covalent inhibition. To test whether inhibited proteasomes are degraded, HeLa cells were pulsed with the covalent and fluorescent proteasome inhibitor MV151 for 2h and chased for three days. Proteasome subunits bound to MV151 are visualized in total lysates by fluorescent scan of a SDS-PAGE gel (Fig 4A). Tubulin staining after protein transfer to a nitrocellulose membrane shows the increasing number of cells during the assay (Fig 4A). The decrease of proteasome-associated MV151 signal in cell lysates, as determined by fluorescent gel scan, showed that inhibited proteasomes are indeed degraded (Fig 4A,B). Whether this degradation is enhanced by (and thus selective for)
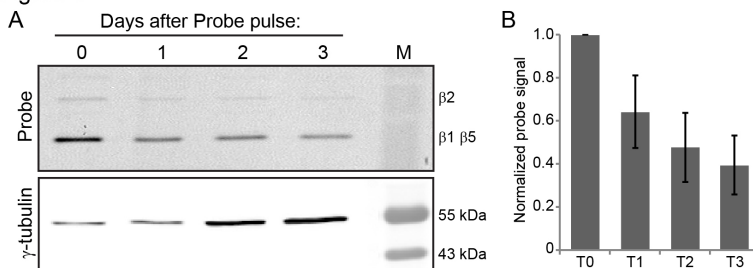
5

Figure 4

Figure 4: Inhibited proteasomes are degraded
A) Fluorescent gel scan of a pulse-chase experiment with the covalent and fluorescent proteasome inhibitor MV151 in HeLa cells. Cells were pulsed for 2h with MV151, washed extensively and chased for three days. Proteasome subunits bound to MV151 are visualized in total lysates by fluorescent scan of a SDS-PAGE gel. Tubulin staining after protein transfer to a nitrocellulose membrane shows the increasing number of cells during the assay. B) Quantification of four independent experiments. Values were normalized to T0 and standard deviations were calculated.

covalent inhibition cannot be concluded since the turnover of un-inhibited proteasomes was not addressed in this experiment. However, the observed decrease in proteasome-associated MV151 signal suggests a half-life of ~2 days, which is shorter than the reported half-life of ~5 days of non-inhibited proteasomes in HeLa cells [26].

Conclusions and Discussion

To maintain sufficient proteasome activity throughout their lifespan, cells are expected to employ quality control mechanisms on the proteasome. Insufficient activity of such mechanisms could result in a pool of damaged proteasomes and may lead to an (age-dependent) decrease in proteasome activity and (harmful) accumulation of damaged proteins. Unraveling the mechanisms underlying proteasome quality control may therefore yield valuable new insights in the process of aging and the onset of age-related diseases like Alzheimer's disease.

An important aspect of proteasome quality control would be the specific degradation of damaged proteasomes. In this study we detected proteasomes in the vacuole of starving budding yeast and in LC3-coated vesicles in HeLa cells. This suggests degradation of the proteasome by the autophagy-lysosome system in these model systems as was also suggested for proteasomes in rat livers [28]. Degradation of another macromolecular complex, the ribosome, has been shown to be mediated by a specific form of macro-autophagy [9]. Whether this is also true for degradation of proteasomes remains unclear, since LC3-containing vesicles are implicated in both macro-autophagy and in several forms of micro-autophagy [7]. Possibly, both types of autophagy are involved like for peroxisomes and mitochondria [8].

For proteasome degradation to be part of quality control it needs to be specific for damaged proteasomes. The observation that only few LC3-containing vesicles contain proteasomes, may suggest specific targeting of proteasomes by autophagy instead of being a bycatch of other (non-specific) autophagic events. Specificity for damaged proteasomes is consistent with the increased internalization of proteasomes upon their covalent inhibition. Pulse-chase experiments with MV151 clearly showed the degradation of inhibited proteasomes. Although the half-life of these proteasomes is lower than has been reported for untreated proteasomes, we cannot claim that this means specificity as we did not study the latter.

Specific degradation of damaged proteasomes implies that the cell can recognize them. This can be mediated by post-translational modifications (PTMs) or associated proteins that mark damaged proteasomes for degradation. A myriad of different PTMs and associated proteins have been assigned to the proteasome [41,42], though as a rule it is unclear whether their presence is damage induced. Age-related PTMs of proteasomes (glycation and conjugation with lipid peroxidation products) are reported in human lymphocytes, though it is unclear whether they signal damage [24]. A more direct link between proteasome damage and PTMs on the proteasome has been reported by Besche *et al*. They reported that *in vivo* and *in vitro* treatment with various proteasome inhibitors leads to selective poly-ubiquitination of a ubiquitin receptor of the 19S (Rpn13) by the proteasome-associated ubiquitin ligase Ube3c/Hul5. Poly-ubiquitination of Rpn13 strongly inhibits the degradation of proteasome substrates, supposedly by occupying the ubiquitin binding sites of the 19S proteasome [43]. The authors suggest that this mechanism evolved to prevent binding of ubiquitinated proteins to (temporarily) impaired proteasomes, but it

may also serve as a mark for the degradation of these impaired proteasomes. Although this is an interesting possibility, the exact signal for degradation of damaged proteasomes remains to be identified.

In this Chapter we present the RITE tool, which seems fit for further study of this degradation signal. In-depth mass spectrometry analysis of old and new proteasomes isolated from dividing yeast cells is likely to yield proteasome modifications that are dependent on the 'age' of the proteasome. These age-dependent modifications are potential degradation signals, but may also give indications for the proteasome damage that induces these signals. Although we recognize the potential of this approach, we considered it outside the scope of this study.

In summary, we can conclude that our data in budding yeast and HeLa cells is consistent with a model of (damaged) proteasome degradation by autophagy and the lysosome. Our data adds two new model systems to the proteasome degradation research and could represent the first sketches of a proteasome quality control system.

Materials and Methods

Yeast strains and growth conditions

The *Saccharomyces cerevisiae* strains used in this study were NKI4103 [33] and an *atg5Δ* derivative of this strain. The atg5 gene knockout was made by PCR-mediated gene disruption based on pRS plasmids [44]. Yeast cells were grown at 30°C in 5 ml liquid YEPD cultures. Unwanted recombination of the RITE cassette was prevented by the addition of Hygromycin B (200 µg/ml, Invitrogen). Liquid cultures were starved by inoculating 5 ml of YEPD with 0.5 ml of an overnight culture followed by 12 days of incubation without medium refreshment. Recombination of the RITE cassette was induced after 2 days of starvation as described by Verzijlbergen *et al* [33].

5

Cell culture and treatments

β1i-GFP overexpressing HeLa cells [37] were cultured in DMEM (Invitrogen) supplemented with 10% FCS and 250 µg/ml Neomycin (BioConnect) under standard culturing conditions. Cells were treated with 50 µM chloroquin (Sigma) to inhibit lysosomal degradation and 100 nM MV151 to inhibit the proteasome. A pulse-chase experiment with MV151 was performed by a 2h incubation of cells with MV151 followed by three PBS washes and the reseeding of the cells in different wells for each time point.

Immunoelectron microscopy

Yeast cells were washed in PBS, fixed for 2h (2% paraformaldehyde and 0.2% glutaraldehyde in 60 mM PIPES, 25 mM HEPES, 2 mM $MgCl_2$, 10 mM EGTA, pH 6.9) and processed for ultrathin cryosectioning [45]. Before immunolabeling, sample sections were blocked by incubation with 0.15 M glycine in PBS for 10 min, followed by 10 min incubation with 1% BSA in PBS. The blocked sections were then incubated with a polyclonal rabbit anti-GFP antibody [46] and a secondary goat anti-rabbit antibody coupled to 10 nm protein-A conjugated colloidal gold (EMlab, University of Utrecht). The immune-stained sections were embedded in uranylacetate and methylcellulose and examined with a Philips CM 10 electron microscope (FEI Eindhoven, The Netherlands).

Microscopy sample preparation and microscopy

To prepare yeast cells for microscopic imaging they were washed in PBS and fixed in 4% formaldehyde for 5 min. The fixed cells were washed, stained with 1 µg/mL Hoechst 33342 (Invitrogen) for 15 min and washed again. Samples were mounted with Vectashield (VectorLaboratories) onto Con A-coated coverslips. HeLa cells were grown on coverslips and fixed for 2 min in 4% formaldehyde or ice-cold methanol. This methanol treatment was also used to permeabilize formaldehyde fixed cells. Fixed and permeabilized cells were blocked at room temperature in 0,5% BSA (Sigma) in PBS for 30-60 min. Blocked cells were incubated for 60 min with rabbit anti-LC3 (Novus Biologicals) in 0.5% BSA, washed with PBS and subsequently incubated for 30 min with goat anti-rabbit coupled to a 647 nm fluorescent dye (Invitrogen). After a final wash step, samples were mounted in Prolong containing DAPI (Life Technologies). Samples were analyzed using a 63x objective on a Leica SP5 confocal microscope, equipped with LAS-AF software (Leica). Single plane images were made using sequential scanning settings and a 405 nm laser for DAPI and Hoechst, 488 nm for GFP labeled proteins, 561 nm for MV151 and 633 nm for secondary antibodies with a 647 nm dye.

Biochemical analysis

Yeast cell lysates were made of 1×10^8 cells, which were washed in cold TE supplemented with 2 mM PMSF and stored at -80°C before further processing. Lysis was performed as described in Terweij et al [47]. Samples were run in a 12% polyacrylamide gel and blotted on a 0.45 µm nitro-cellulose membrane. Membranes were blocked with 4% skim milk powder (Oxoid) in PBS + 0.1% Tween. Primary antibody incubations were performed at RT for 1h in blocking buffer using mouse anti-3-PGK (1:5000, Invitrogen) and rabbit anti-GFP or rabbit anti-mRFP (1:2000; 46). Secondary antibody staining was performed for 45 min at RT using the goat anti-rabbit (700 nm) and the goat anti-mouse (800 nm) LI-COR Odyssey IRDyes (1:10.000; LI-COR). Membranes were scanned with a LI-COR Odyssey IR Imager (Biosciences) and analyzed with the associated software package.

HeLa cells were lysed in 1x sample buffer with 5% β-mercaptoethanol and subsequently sonicated and boiled for 5 min at 96°C. HeLa lysates were separated on gel as described for the yeast cell lysates. A fluorescence scan was made of the gel on a ProXpress fluorescence scanner (Perkin Elmer), using 550/30 nm excitation and 590/35 nm emission. Gels were blotted and blocked as described before and stained with mouse anti-tubulin (1:5000; Sigma) and the goat anti-mouse (700 nm) LI-COR Odyssey IRDye (LI-COR; 1:10.000).

References

1. Hartl, F. U., Bracher, A. & Hayer-Hartl, M. Molecular chaperones in protein folding and proteostasis. Nature 475, 324–32 (2011).

2. Balch, W. E., Morimoto, R. I., Dillin, A. & Kelly, J. W. Adapting proteostasis for disease intervention. Science 319, 916–9 (2008).

3. Vilchez, D., Saez, I. & Dillin, A. The role of protein clearance mechanisms in organismal ageing and age-related diseases. Nat. Commun. 5, 5659 (2014).

4. Schmidt, M. & Finley, D. Regulation of proteasome activity in health and disease. Biochim. Biophys. Acta 1843, 13–25 (2014).

5. Ciechanover, A. Intracellular protein degradation: from a vague idea through the lysosome and the ubiquitin-proteasome system and onto human diseases and drug targeting. Bioorg. Med. Chem. 21, 3400–10 (2013).

6. Feng, Y., He, D., Yao, Z. & Klionsky, D. J. The machinery of macroautophagy. Cell Res. 24, 24–41 (2014).

7. Li, W., Li, J. & Bao, J. Microautophagy: lesser-known self-eating. Cell. Mol. Life Sci. 69, 1125–36 (2012).

8. Reggiori, F. & Klionsky, D. J. Autophagic processes in yeast: mechanism, machinery and regulation. Genetics 194, 341–61 (2013).

9. Kraft, C., Deplazes, A., Sohrmann, M. & Peter, M. Mature ribosomes are selectively degraded upon starvation by an autophagy pathway requiring the Ubp3p/Bre5p ubiquitin protease. Nat. Cell Biol. 10, 602–10 (2008).

10. Tomko, R. J. & Hochstrasser, M. Molecular architecture and assembly of the eukaryotic proteasome. Annu. Rev. Biochem. 82, (2013).

11. Chen, P. & Hochstrasser, M. Biogenesis, structure and function of the yeast 20S proteasome. EMBO J. 14, 2620–30 (1995).

12. Liu, C.-W. & Jacobson, A. D. Functions of the 19S complex in proteasomal degradation. Trends Biochem. Sci. 38, 103–10 (2013).

13. Hershko, a & Ciechanover, a. The ubiquitin system for protein degradation. Annu. Rev. Biochem. 61, 761–807 (1992).

14. Glickman, M. H. & Ciechanover, A. The Ubiquitin-Proteasome Proteolytic Pathway : Destruction for the Sake of Construction. Physiol. Rev. 82, 373–428 (2002).

15. Carrard, G., Bulteau, A.-L., Petropoulos, I. & Friguet, B. Impairment of proteasome structure and function in aging. Int. J. Biochem. Cell Biol. 34, 1461–1474 (2002).

16. Dasuri, K. et al. Aging and dietary restriction alter proteasome biogenesis and composition in the brain and liver. Mech. Ageing Dev. 130, 777–83 (2009).

17. Lee, C., Klopp, R. G., Weindruch, R. & Prolla, T. A. Gene Expression Profile of Aging and Its Retardation by Caloric Restriction. Science (80-.). 285, 1390–1393 (1994).

18. Vernace, V. A., Arnaud, L., Schmidt-glenewinkel, T. & Figueiredo-, M. E. Aging perturbs 26S proteasome assembly in Drosophila melanogaster. Faseb J 21, 2672–2682 (2012).

19. Chen, Q., Thorpe, J., Dohmen, J. R., Li, F. & Keller, J. N. Ump1 extends yeast lifespan and enhances viability during oxidative stress: central role for the proteasome? Free Radic. Biol. Med. 40, 120–6 (2006).

20. Kruegel, U. et al. Elevated proteasome capacity extends replicative lifespan in Saccharomyces cerevisiae. PLoS Genet. 7, e1002253 (2011).

21. Chondrogianni, N., Petropoulos, I., Franceschi, C., Friguet, B. & Gonos, E. . Fibroblast cultures from healthy centenarians have an active proteasome. Exp. Gerontol. 35, 721–728 (2000).

22. Aragon, A. D. et al. Characterization of differentiated quiescent and nonquiescent cells in yeast stationary-phase cultures. Mol. Biol. Cell 19, 1271–80 (2008).

23. Bajorek, M., Finley, D. & Glickman, M. H. Proteasome Disassembly and Downregulation Is Correlated with Viability during Stationary Phase. Curr. Biol. 13, 1140–1144 (2003).

24. Carrard, G., Dieu, M., Raes, M., Toussaint, O. & Friguet, B. Impact of ageing on proteasome structure and function in human lymphocytes. Int. J. Biochem. Cell Biol. 35, 728–739 (2003).

25. Glockzin, S. Activation of the Cell Death Program by Nitric Oxide Involves Inhibition of the Proteasome. J. Biol. Chem. 274, 19581–19586 (1999).

26. Hendil, K. B. The 19 S multicatalytic "prosome" proteinase is a constitutive enzyme in HeLa cells. Biochem. Int. 17, 471–478 (1988).

27. Tanaka, K. Half-Life of Proteasomes (Multiprotease Complexes) in Rat Liver '. Biochem. Biophys. Res. Commun. 159, 1309–1315 (1989).

28. Cuervo, M., Palmer, A., Rivett, J. & Knecht, E. Degradation of proteasomes by lysosomes in rat liver. Eur. J. Biochem. 227, 792–800 (1995).

29. Balaban, R. S., Nemoto, S. & Finkel, T. Mitochondria, oxidants, and aging. Cell 120, 483–95 (2005).

30. Arrigo, A. ., Tanake, K., Goldberg, A. L. & Welch, W. J. Identity of the 19S "prosome" particle with the large multifunctional protease complex of mammalian cells (the proteasome). Nature 331, 192–194 (1988).

31. Price, J. C., Guan, S., Burlingame, A., Prusiner, S. B. & Ghaemmaghami, S. Analysis of proteome dynamics in the mouse brain. PNAS 107, 14508–14513 (2010).

32. Van Deventer, S. J., Menendez-Benito, V., van Leeuwen, F. & Neefjes, J. N-Terminal Acetylation And Replicative Age Affect Proteasome Localization And Cell Fitness During Aging. J. Cell Sci. (2014).

33. Verzijlbergen, K. F. et al. Recombination-induced tag exchange to track old and new proteins. PNAS 107, 64–68 (2010).

34. Gray, J. V et al. Sleeping Beauty : Quiescence in Saccharomyces cerevisiae. Microbiol. Mol. Biol. Rev. 68, 188–202 (2004).

35. Cheong, H. et al. Atg17 Regulates the Magnitude of the Autophagic Response. Mol. Biol. Cell 16, 3438–3453 (2005).

36. Laporte, D., Salin, B., Daignan-Fornier, B. & Sagot, I. Reversible cytoplasmic localization of the proteasome in quiescent yeast cells. J. Cell Biol. 181, 737–45 (2008).

37. Reits, E., Benham, M., Plougastel, B., Neefjes, J. & Trowsdale, J. Dynamics of proteasome distribution in living cells. EMBO J. 16, 6087–94 (1997).

38. Klionsky, D. J., Cuervo, A. M. & Seglen, P. O. Methods for Monitoring Autophagy from Yeast to Human. Autophagy 3, 181–206 (2007).

39. Seglen, P. O., Grinde, B. & Solheim, a E. Inhibition of the lysosomal pathway of protein degradation in isolated rat hepatocytes by ammonia, methylamine, chloroquine and leupeptin. Eur. J. Biochem. 95, 215–225 (1979).

40. Verdoes, M. et al. A fluorescent broad-spectrum

5

proteasome inhibitor for labeling proteasomes *in vitro* and *in vivo*. Chem. Biol. 13, 1217–26 (2006).

41. Leggett, D. S. *et al*. Proteasome Structure and Function. Mol. Cell 10, 495–507 (2002).

42. Wang, X. *et al*. Mass Spectrometric Characterization of the Affinity-Purified Human 26S Proteasome Complex. Biochemistry 46, 3553–3565 (2007).

43. Besche, H. C. *et al*. Autoubiquitination of the 26S Proteasome on Rpn13 Regulates Breakdown of Ubiquitin Conjugates. EMBO J. 33, 1159–1176 (2014).

44. Brachmann, C. B. *et al*. Designer deletion strains derived from *Saccharomyces cerevisiae* S288C: A useful set of strains and plasmids for PCR-me-diated gene disruption and other applications. Yeast 14, 115–132 (1998).

45. Calafat, B. J. *et al*. Human Monocytes and Neutrophils Store Transforming Growth Factor-a in a Subpopulation of Cytoplasmic Granules. Blood 90, 1255–1267 (1997).

46. Rocha, N. *et al*. Cholesterol sensor ORP1L contacts the ER protein VAP to control Rab7-RILP-p150 Glued and late endosome positioning. J. Cell Biol. 185, 1209–25 (2009).

47. Terweij, M. *et al*. Recombination-induced tag exchange (RITE) cassette series to monitor protein dynamics in *Saccharomyces cerevisiae*. G3 3, 1261–72 (2013).
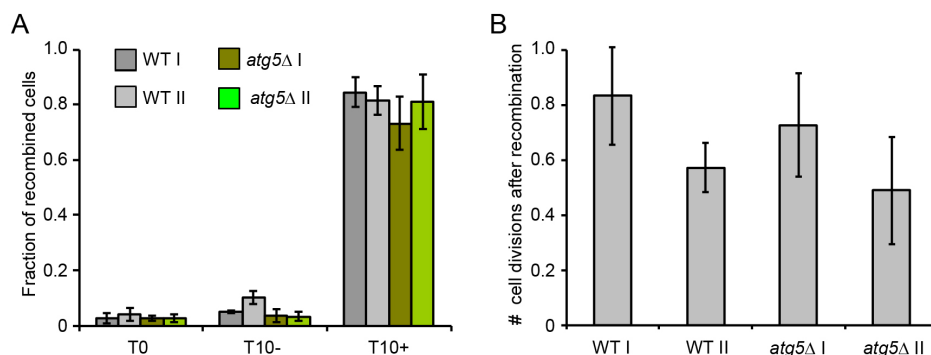
Supplemental Figures:

Figure S1

Figure S1: WT and autophagy-deficient cells have similar recombination and growth characteristics
A) Fraction of cells with a recombined RITE cassette as determined by plating assay [33]. Limited non-induced recombination can be observed before recombination is induced (T0) and ten days after that without recombination (T10-). Hormone-induced recombination can be observed ten days after the recombination event (T10+). Non-induced and hormone-induced recombination is not significantly different for WT and autophagy-deficient cells. Values and standard deviations are based on a biological triplicate. B) The number of cell divisions between the time of the recombination (T0) and the end of the experiment (T10) was assessed by FACS-based cell counting. No significant differences were observed between WT and autophagy-deficient cells. Values and standard deviations are based on a biological triplicate.

5